Dielectric Properties Characterization from 0.5 to 50 GHz of Breast Cancer Tissues

Andrea Martellosio, *Student Member, IEEE*, Marco Pasian, *Senior Member, IEEE*, Maurizio Bozzi, *Senior Member, IEEE*, Luca Perregrini, *Fellow, IEEE*, Andrea Mazzanti, *Senior Member*, *IEEE*, Francesco Svelto, *Fellow*, *IEEE*, Paul Eugene Summers, Giuseppe Renne, Lorenzo Preda, and Massimo Bellomi

***Abstract*— Knowledge of the dielectric properties of human tissues is important for several biomedical applications, including imaging and hyperthermia treatment, as well as for determining safety thresholds in policy making. Breast tissues, both normal and tumorous, are of particular interest because of the medical and social impact of breast cancers. While experimental data is available up to 20 GHz, for higher frequencies this information is missing, or has been extrapolated from models based on lower-frequency data. Emerging technologies and applications in the mm-wave region would benefit from experimental data that bridge this gap.**

This paper presents the characterization of dielectric properties of breast tissues for the frequency range from 0.5 to 50 GHz. Cole-Cole models are derived for normal and tumorous tissues based on experimental measurements on more than 220 tissue samples obtained at surgery (*ex-vivo*) from a population exceeding 50 patients, covering a wide span of normal and tumorous tissues, from patients ranging in age from 28 to 85 years, with a time from excision to measurements under 3.5 hours.

This paper also presents a comprehensive analysis of the differences between normal and tumorous breast tissues at different frequencies in terms of sensitivity and specificity.

***Index Terms*—Biomedical applications, breast cancer, dielectric characterization, dielectric properties, ex-vivo tissues, microwave imaging, mm-waves, sensitivity, specificity.**

I. Introduction

THE USE of mm-waves in biomedical applications has been increasing in recent years, and in many cases it represents a natural continuation of well established developments in the RF and microwave region of the electromagnetic spectrum [1]. The natural advantage of mm-waves compared to microwaves is the shorter wavelength, which allows better spatial resolution and downscaling of components (in particular sensors and antennas). In addition, the latest developments in mm-wave technologies, driven by the automotive (car radar), safety (body scanner), and communication (short-range links) markets, are a significant stimulus for the exploitation of mm-waves in other fields [2]–[4]. Biomedical applications benefiting from this technological trend cover many different aspects, including imaging of outer organs [5], localized near-skin hyperthermia medical hyperthermia [6], *in-vivo* and *ex-vivo* sensing devices (glucose, corneal, dental caries, and skin cancer monitoring) [7]–[10], and also stimulated discussions on the compliance with exposure guidelines [11].

The potential for mm-waves to contribute to breast cancer detection and characterization deserves particular attention because of the high societal impact, and the ongoing debate over existing screening practices for this type of cancer. Breast cancer detection is currently achieved (on top of manual palpation) by using three different imaging techniques, i.e., ultrasound, magnetic resonance imaging, and X-ray mammography. However, all techniques have disadvantages. Ultrasound is strongly dependent on physician ability, thus generating an extremely variable success rate. Magnetic resonance imaging involves a time-consuming procedure with a large and costly machine, preventing its use for mass periodical screening. In addition, the use of a contrast agent, which allows to improve the evaluation of the neoplastic and inflammatory pathologies, make it an invasive procedure. X-ray mammography, on the other hand, is widely used for mass periodical screening because it provides good diagnostic performance at relatively low cost, but requires an uncomfortable compression of the breast and exposure to ionizing radiation, which augments the risk of tumour development with the increase of repeated screening. Regardless of the diagnostic modality, biopsy is widely used to obtain a final determination of the nature of lesions before proceeding to intervention, which typically involves surgery.

For the above reasons, alternative or complementary low-cost approaches based on non-ionizing electromagnetic waves are welcome and could have a significant clinical impact on two major applications. The first application concerns breast imaging. Prototypes systems for breast imaging based on

Manuscript received January 27, 2016. This work was partially supported by the Italian Association for Cancer Research (AIRC).

A. Martellosio, M. Pasian, M. Bozzi, L. Perregrini, A. Mazzanti, F. Svelto are with the Department of Electrical, Computer and Biomedical Engineering, University of Pavia, Pavia, Italy (e-mail: andrea.martellosio01@ateneopv.it, marco.pasian@unipv.it; maurizio.bozzi@unipv.it; luca.perregrini@unipv.it; andrea.mazzanti@unipv.it; francesco.svelto@unipv.it).

P. E. Summers is with the Department of Radiology, European Institute of Oncology, Milano, Italy (email: paul.summers@ieo.it).

G. Renne is with the Department of Pathology and Laboratory Medicine, European Institute of Oncology, Milano, Italy (email: giuseppe.renne@ieo.it).

L.Preda is with the Department of Radiology, European Institute of Oncology, Milano, Italy, and with the Department of Clinical-Surgical, Diagnostic and Pediatric Sciences, University of Pavia, Pavia, Italy, and with the National Center of Oncological Hadrontherapy (CNAO Foundation), Pavia, Italy (email: lorenzo.preda@unipv.it).

M. Bellomi is with the Department of Radiology, European Institute of Oncology, Milano, Italy, and with the Department of Oncology, University of Milano, Milano, Italy (email: massimo.bellomi@ieo.it).

microwaves up to few gigahertz have been demonstrated [13]–[17], but these lack spatial resolution [12], [18]. Therefore, imaging systems at higher frequencies, including mm-waves, THz-waves, and even infrared frequencies, have been proposed to improve resolution, overcoming the limited penetration depth typical of these frequencies mainly using suitable array architectures [19]–[23]. The second application is related to tissue identification (normal vs. lesion), both for *ex-vivo* (after biopsy) and *in-vivo* (directly during surgery) scenarios. In these cases, the penetration depth is not a major issue, and prototypes for cancer identification have been developed in the THz and sub-THz regime [24].

In parallel with these developments, the rapidly growing use of high-frequency communication systems, mainly intended for short-range and indoor links between devices, and automotive radars, has created a need to verify the compliance of these systems with respect to allowed exposure thresholds, as well as the consistency of said thresholds with the health protection priorities of policy-makers [11].

A limitation for the development of mm-wave applications is that the complex permittivity of human breast tissues has been experimentally measured only up to 20 GHz and above 150 GHz [25]–[28]. Traditionally, the dielectric properties for mm-wave frequencies have been extrapolated using models based on the sub-20-GHz data, and to the knowledge of the authors, not been verified with experimental measurements. Such measurements are fundamental in the bioengineering domain to verify whether mm-waves are valid candidates for tumour identification and more generally to accelerate the development of new sensors and applications [1].

This paper aims to fill the gap in knowledge of dielectric properties for frequencies up to 50 GHz, by establishing a comprehensive catalogue of breast tissue characteristics that extend a preparatory work presented, where different types of animal tissues (i.e., lean and fat tissues) are compared with first preliminary samples of a human breast (i.e., malignant and normal tissues) [29]. Surgical breast tissues, obtained from 53 patients, for a total of 222 different samples, are characterized in terms of complex permittivity and validated by pathological analysis. The population covers a wide range of ages (from 28 to 85 years), time from excision to measurement (from 6 minutes to 3 hours and 29 minutes), and normal and tumorous tissues (166 and 56, respectively), thus providing an overview of breast pathology.

This extensive experimental campaign, described in Section II and III, allows us to derive Cole-Cole models for breast tissues from 0.5 to 50 GHz, reported in Section IV. In addition, the differences between normal and tumorous breast tissues are analyzed for various frequencies to provide estimates of the potential sensitivity and specificity, as defined in Section V.

II. Measurement Setup and Workflow

The measurement setup, depicted in Fig. 1, is based on an open-ended coaxial probe. This approach, which provides the complex dielectric permittivity of the material under test (MUT) after measuring the complex reflection coefficient, is particularly suited for the broadband characterization of biological tissues obtained at surgery. The small footprint of the coaxial probe head, less than one centimetre in diameter, and the working principle, a reflectometry technique requiring only a small pressure between the coaxial probe head and the MUT, are well suited to work with small biological samples that cannot be specifically prepared for dielectric characterization [30]. Indeed, the subsequent use of the same biological sample for pathological analysis requires rapid and non-destructive measurements.

The system shown in Fig. 1 is composed of an open-ended coaxial probe (Keysight 85070E Dielectric Probe Kit), suitable for measurements over the 0.5–50 GHz frequency range. The coaxial probe is driven by a Keysight E8361C Vector Network Analyzer (VNA) via a high-performance flexible coaxial cable, which is also used to retrieve, display and store the complex dielectric permittivity of the MUT. The mechanical part consists of a positioner to support the probe over the MUT, and a mechanical mover on which the MUT is placed, in such a way that it can be moved toward the coaxial probe, fixed at the mechanical positioner, achieving a repeatable pressure, avoiding air gaps and MUT deformations.

The system is conceived to provide the maximum stability to the MUT characterization. At frequencies approaching 50 GHz, phase stability is important for reliable measurements. The high-performance flexible coaxial cable, provided with the Keysight 85070E Dielectric Probe Kit, is specifically designed to provide phase stability against cable movements [31]. Moreover, the cable, supported by the mechanical positioner, remains untouched during the entire experimental characterization, as the MUT is moved toward the coaxial probe using the mechanical mover, and not vice-versa. In addition, the mechanical mover is equipped with a digital pressure sensor to provide a controlled and repeatable pressure, in the range of few tens of milligrams. The coaxial probe is calibrated before each measurement using standard loads, namely distilled water, short circuit, and open ended. The coaxial probe head exhibits a small sensing area. In particular, the diameter of the inner conductor is 0.268 mm while the diameter of the outer conductor is 1.6 mm.

To increase probe robustness and improve probe handling, the coaxial probe is housed in an external aluminium body, not contributing to the sensing area, which is slightly less than one centimetre in diameter.

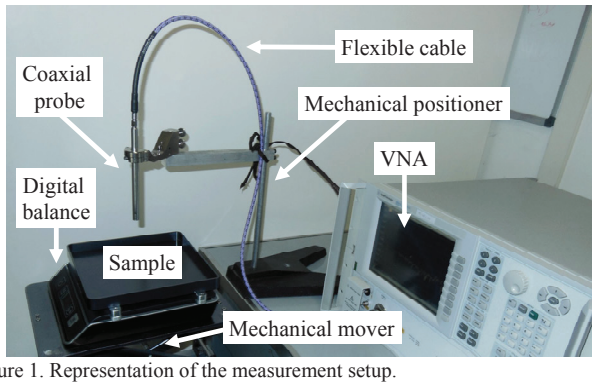

Figure 1. Representation of the measurement setup.

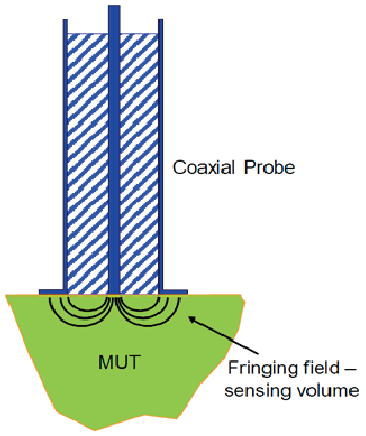

Figure 2. Schematic representation of the coaxial probe sensing volume. The outer aluminium body is not depicted.

Thus, the probe generates a quasi-static capacitor-like field with a sensing volume described by a diameter and a penetration depth of around 2 mm for all operation frequencies (Fig. 2). However, this sensing volume is not uniformly weighted by the probe to calculate the dielectric permittivity. Instead, the portion of the sensing volume close to the probe head is more relevant than other areas [31]. For this reason, a lot of attention is paid to have a MUT as uniform as possible for each measuring area, in such a way that the volume immediately beneath the probe head is representative of the entire sensing volume.

Before the experimental measurements on human biological samples, the coaxial probe was verified in terms of accuracy and sensing volume, taking into account the probe dielectric properties chart, shown in Fig. 3. Measurements on different materials with known dielectric properties, including liquids (deionized water [32, 33], methanol [33], ethanol [33], 2-propanol [34], and n-butanol [33]), and solids (black foam, preperm L700HF, and Teflon [35]), were used to estimate the accuracy. As an example, the measurement of deionized water at 25°C (a material with large values for both the real and the imaginary part of the dielectric permittivity, well within the recommend region of the probe chart) and Teflon (a material with small values for both the real and the imaginary part of the dielectric permittivity, an extreme low-loss case in the non-recommend region of the probe chart, where the measurement of the imaginary part is practically impossible) are reported in Fig. 4, showing excellent agreement with the theoretical values.

In addition, the sensing volume was evaluated through measurements of several materials (the liquids mentioned above, as well as agarosio, lard, bacon, coppa, pork filet, chicken heart, liver, and breast), varying the sample thickness, and calculating the measurement variation with and without a metal plate below the MUT. Varying the sample thickness, and consequently the distance between the probe head and the metal plate, it is possible to determine when the latter ceases to affect the measurements, thus providing a metric of the maximum penetration depth. As an example, in Fig. 5 it is shown the percentage variation of the real part of dielectric permittivity for a liquid (deionized water at 25 °C, similar to human lean tissues) and for a biological sample (lard, similar to human fat tissues). The variation is negligible (i.e., lower than 1%) for distances greater than or equal to 2 mm.

Sensing on the lateral direction, this is largely dictated by the probe geometry, as the field is practically confined between the outer (1.6 mm) and the inner conductor. A previous work [31], considering known standard liquids, indicated sensing diameters in the order of 5 mm and 7 mm for a 2.2-mm and 3-mm probe, respectively. However, during the preparatory experimental campaign discussed above, a lateral sensing diameter of 2 mm is retrieved, being any effect on the measurement of the dielectric permittivity given by outer regions negligible compared with the expected variability of biological tissues.

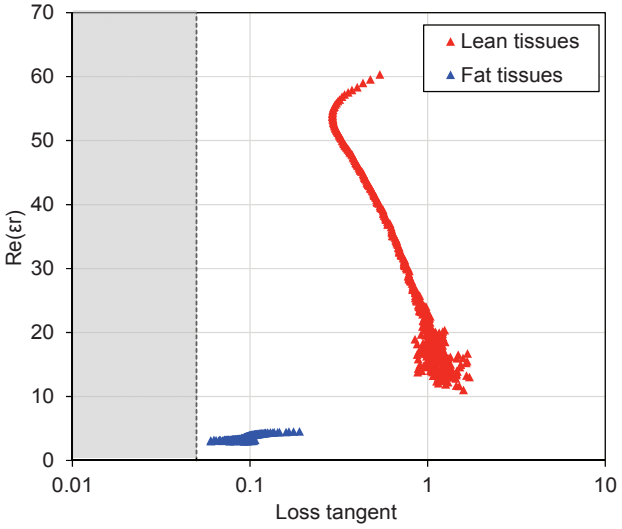

Figure 3. Dielectric properties chart for lean and fat animal tissues from 0.5 GHz to 50 GHz against the coaxial probe range of usability provided by the probe manufacturer (non-recommended region shown in shaded grey).

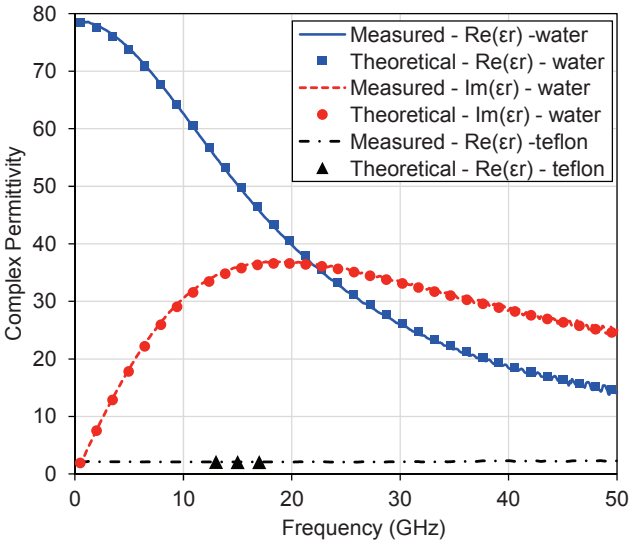

Figure 4. Accuracy of the measurement evaluated for a liquid sample (deionized water at 25°C) and a solid sample (Teflon). Comparison between measured and theoretical values.

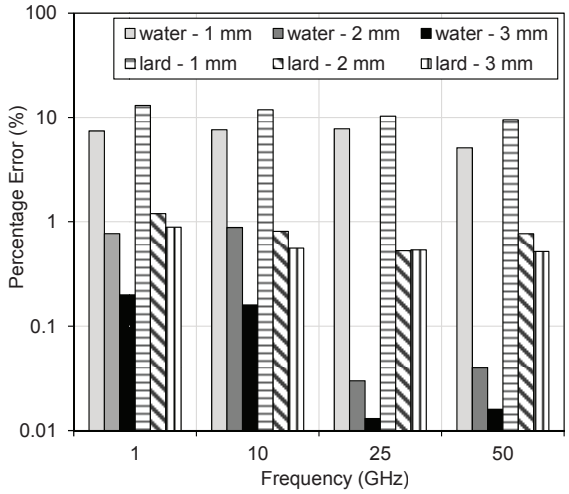

Figure 5. Volume sensing of the measurement evaluated for a liquid sample (deionized water at 25°C) and a biological sample (lard). Percentage error, of the real part of complex permittivity, calculated for several distances between the probe and the sample under measurement.

In any case, mechanical limitations given by the external probe body practically dictated to work with spots not smaller than 5-6 mm in diameter. These preliminary experimental phases confirmed the performance of the coaxial probe over the entire 0.5–50 GHz band. In particular, the dielectric properties of both lean and fat animal tissues lay outside the *non-recommended* region provided by the probe manufacturer, as shown in Fig. 3. Since lean and fat animal tissues are expected to provide a response similar to tumorous and normal human breast tissues, respectively, this preliminary verification suggests the probe is appropriate for human tissues.

The measurements on human tissues took place at the European Institute of Oncology (IEO) in Milan, Italy. The clinical protocol is outlined in Fig. 6, and was defined in close collaboration with the medical staff in order to optimize the integration of the electromagnetic measurements into the standard medical routine leading from surgery to pathological analysis.

The surgical specimen (lumpectomy, quadrantectomy or mastectomy, including neoplasm and surrounding normal tissue) were sent to the surgical pathology gross room where they were labelled and handled by the pathologist. From each surgical excision, a roughly parallelepiped sample was prepared by the pathologist from an area suspected to neoplastic (related to the development of tumours) and normal tissue based on gross appearance. These samples had a thickness of about 6 mm and volume of between 700 mm^3 and 1500 mm^3 in order to ensure full contact between the sample and sensitive region of the probe head and to ensure all subsequent pathological analysis (as shown in Fig. 7, where an example of a 6x15x15 mm^3 tumour sample is represented). The time range between surgical excision and measurement was recorded. Depending on the pathologists workload at the gross stations, and on the complexity of the surgical specimens, this time range varied from 6 minutes to 3 hours and 29 minutes. The temperature of the sample was measured using a contact-less high-precision infrared thermometer immediately prior to dielectric permittivity characterization. Temperature and humidity stability of the sample, was guaranteed by using bio-specimen transport bags (from which the specimen was removed around one minute before the electromagnetic characterization, which takes a few seconds) and by air conditioned system of pathology gross rooms, similar to that of surgical theatre. Overall, this procedure allows for partly approaching the humidity condition typical of *in-vivo* tissues, which provide higher values for both the real and imaginary part compared to *ex-vivo* tissues [36].

The number of sites subjected to dielectric constant measurement, marked with different acrylic inks, depended on the size of the sample (Fig. 8). These inks demarcated areas are easily recognized on microscopic examination. During this phase, the engineer evaluates each digital image acquired by the microscope and indicates, for each measurement point, the area to be analyzed by the pathologist. An example of microscope image of a slice is shown in Fig. 9, in which the difference between healthy cells and neoplastic cells can be appreciated through the pink and purple hues respectively. After normal pathologic workflow, all the individual areas measured, have been reviewed by a pathologist, on digital images, limiting the dichotomous distinction between tumour and normal tissue (Fig. 9). The histological "diagnoses" were used to establish a database where the dielectric properties of each area of the samples, from 0.5 GHz to 50 GHz, together with the sample site.

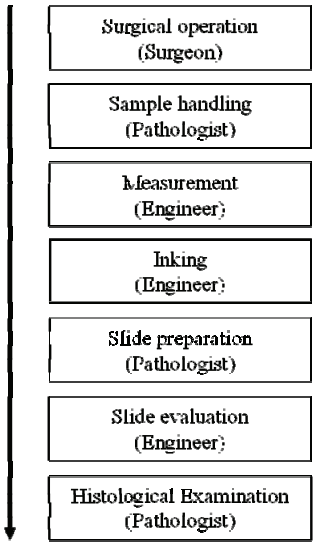

Figure 6. Clinical protocol agreed between medical and engineering staff.

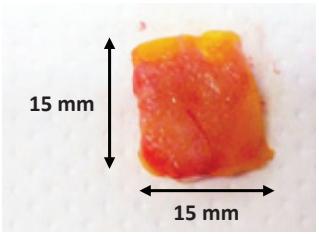

Figure 7. Example of breast tumorous tissue.

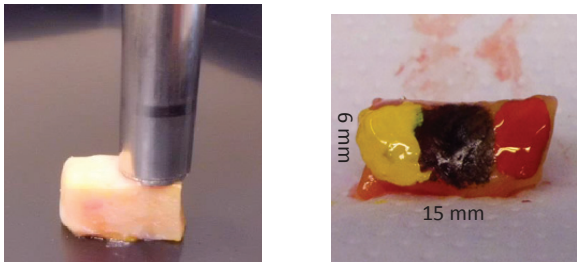

(*a*) (*b*)

Figure 8. Example of dielectric permittivity characterization for human biological samples, showing: (*a*) the head of the coaxial probe in contact with a sample of a breast obtained at surgery; (*b*) the use of acrylic inks to easily identify the spot measurements for the subsequent pathological analysis.

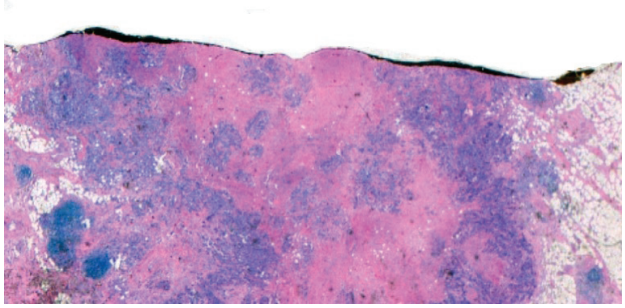

Figure 9. Example of microscope image of a slice of a human biological sample prepared for the pathological analysis. The acrylic inks are visible as the dark spots at the upper margin of the sample.

III. Dielectric Properties of Breast Cancer Tissues

The dielectric properties of breast tissues measured following the clinical protocol presented in section II are described in terms of real and imaginary part. The experimental campaign lasted two months and it included 53 different patients, providing 222 different samples. The pathological features are used as the standard of reference in assessing the ability of dielectric properties to discriminate between the tumorous and normal tissues. A further analysis is made within each tissue type. In particular, tumorous tissues are classified as invasive or non-invasive, while normal tissues are classified as low, medium, or high density tissues. In addition, the effects of patient age, sample temperature, and time between excision and measurements are analysed in order to evaluate their possible influence.

A. Dielectric differences between tissues

On the basis of the pathological analysis, measurements related to normal (166 samples) and tumorous tissues (56 samples) are plotted versus frequency for both the real (Fig. 10) and imaginary (Fig. 11) parts of the complex relative permittivity. For each sample, five consecutive measurements were taken to verify the stability over time (a time of 3 seconds elapses between consecutive measurements). In all cases, a practically perfect overlap was achieved. An example of this superposition is shown in Fig. 12 and in Fig. 13, demonstrating the repeatability of the measurement setup, in particular against possible variation of the contact pressure. In particular, the optimum pressure for stable results using our measurement setup is in the order of 14 kPa (around 140 g/cm^2). This calibration procedure was part of the preparatory experimental campaign on animal tissues and other known materials, which allowed for acquiring the required know how. This pressure guarantees a good contact between the probe and the sample, avoid air bubbles or excessive compression.

The measured samples differed from each other in terms of water and fat content, as detailed later in this section. This is reflected into a wide variability of the relative permittivity, as shown in Fig. 10 and Fig. 11. To provide a clear overview of this variability, Fig. 14 and Fig 15 summarize the measured data for both normal and tumorous tissues in terms of mean values (solid lines) and standard deviation (shaded bands, 1 sigma). It can be observed that the mean values for tumorous and normal tissues are separated from each other at all frequencies, both for the real and imaginary part, with negligible overlap of the first standard deviation of the distributions. From a biophysical point of view, the predominant polarization effect in tissues between 0.5 GHz and 50 GHz is due to the orientation mechanism of water molecules. It is clear therefore that the observed differences in relative dielectric permittivity reflect difference in water content between tumour and normal breast tissue.

In this particular case, three mechanisms may be involved in elevating the water content of tumours. First, edema in the tumour region may augment the extra-cellular water content. Second, tumour areas are unlikely to have large intracellular fat content, whereas adipose tissue, with relatively low intracellular water content, is a significant feature in breasts.

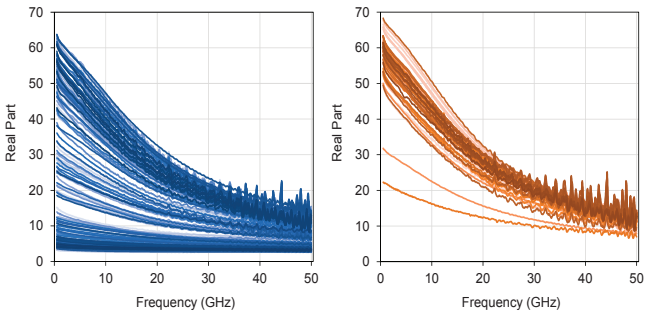

(*a*) (*b*)

Figure 10. Measurements of the real part of the complex relative permittivity for normal (a) and tumorous tissues (b).

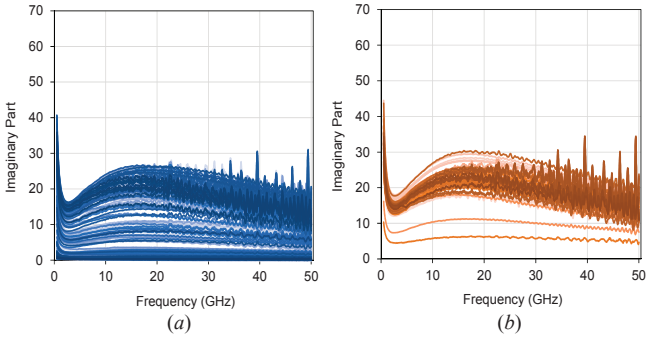

(*a*) (*b*)

Figure 11. Measurements of the imaginary part of the complex relative permittivity for normal (a) and tumorous tissues (b).

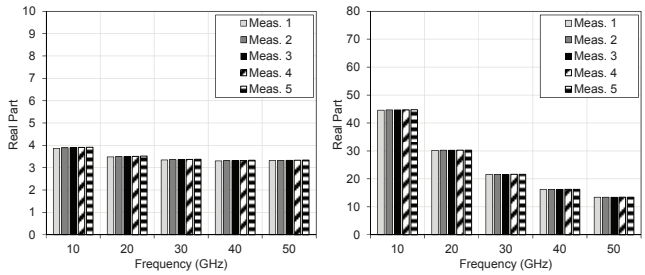

(*a*) (*b*)

Figure 12. Example of five consecutive measurements of the real part of the complex relative permittivity. Example reported for (*a*) normal and (*b*) tumorous tissues.

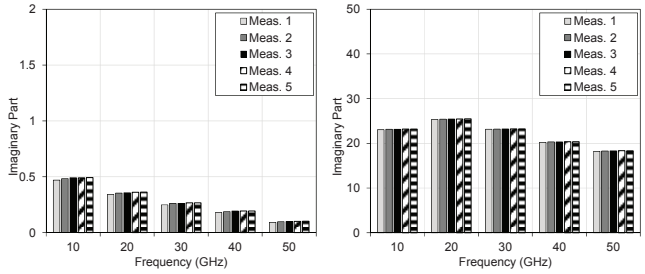

(*a*) (*b*)

Figure 13. Example of five consecutive measurements of the imaginary part of the complex relative permittivity. Example reported for normal (*a*) and tumorous tissues (*b*).

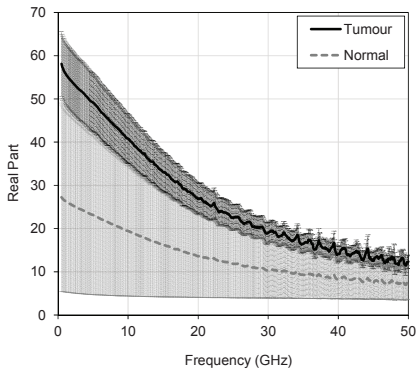

Figure 14. Characterization of the real part of the relative dielectric permittivity for normal and tumorous tissues. The black solid line depicts the average for tumorous tissues whereas the grey dashed line depicts the average for normal tissues. The shaded region denotes the variable range at ± 1 standard deviation.

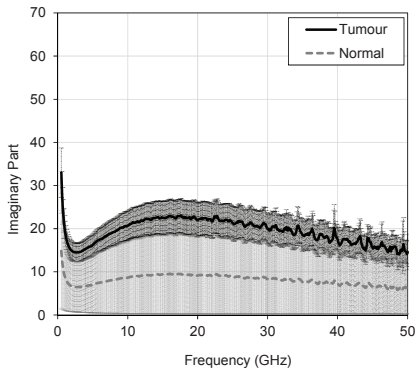

Figure 15. Characterization of the imaginary part of the relative dielectric permittivity for normal and tumorous tissues. The black solid line depicts the average for tumorous tissues whereas the grey dashed line depicts the average for normal tissues. The shaded region denotes the variable range at ± 1 standard deviation.

Figure 16. Two samples of normal tissues. On the left a photograph of a high adipose tissue and on the right a photograph of a low adipose tissue.

TABLE I – DIFFERENT GROUPS FOR THE NORMAL TISSUES

Group	*Adipose content (%)*
High adipose (Low density)	80 - 100
Intermediate adipose (Medium density)	20 - 80
Low adipose (High density)	0 – 20

Lastly, tumorous tissues are often accompanied by a neoangiogenesis and therefore a greater vascular water content. It is also notable that normal tissues exhibit a much wider range of values than tumorous tissues. In fact, as seen in Fig. 14 and in Fig. 15, the standard deviations for normal tissues is roughly twice that of tumorous tissues. Heterogeneity in the adiposity of the normal tissues (also referred to as breast density) appears to account for this observation as examined in the next section.

The large number of experimental samples (> 200), allows for a limited dispersion of the data. Both the 95% and 99% confidence intervals are very stable over the frequency range 0.5–50 GHz. Indeed, for the 95% confidence interval, the minimum, average, and maximum width of the confidence interval is ±9.5%, ±10.5%, and ±11.9% of the mean, respectively. For the 99% confidence interval, the minimum, average, and maximum width of the confidence interval is ±10.0%, ±11.1%, and ±13.0% of the mean, respectively.

B. Dielectric differences within tissues

Amongst the tumorous tissues, both invasive and non-invasive tumours are identified by pathologist, but between them no statistical difference in dielectric properties is observed. Amongst the normal tissues, pathology reveals a wide range of adiposity.

As described in Table I, the normal tissue samples are divided into three sub-groups on the basis of their percentage of adipose component. Of the 166 samples, 74 corresponded to tissues characterized by a high adipose content (80% ─ 100%). Tissues characterized by a low adipose content (0% ─ 20%), generally composed primarily of a mixture of fibrous and glandular tissue, accounted for 62 samples. The remaining 30 samples are characterized by an intermediate adipose content (20% - 80%). The photographs in Fig. 16 show (left) a high adipose content tissue and (right) a low adipose content tissue. As fat content decreases, the average dielectric properties rise significantly between groups (Fig. 17), both for the real part and the imaginary part of the complex relative permittivity. For the real part, the effect is most pronounced at low frequencies where the values for the low adipose tissues (square markers) are 3-5 times greater than high adipose tissues (circle markers). Conversely, for the imaginary part the

effect is accentuated around 20 GHz where a resonance frequency of the water molecules has been reported previously. These differences appear to explain the wide variability of the dielectric properties of normal tissues.

C. Comparison between different types of normal tissues and tumorous tissues

The dependence of dielectric properties on breast water density in healthy breast tissues suggests that the contrast between tumorous and normal tissues will depend on the nature of the tissue surrounding the tumour. To examine the differences between tumour and normal tissues as a function of breast density, the average complex relative permittivity is compared between tumour and the three breast density groups at multiple frequencies, as depicted in Fig. 18 (real part) and in Fig. 19 (imaginary part). Between tumorous and low density tissues an average difference of 70% and 80% exists for the real and the imaginary part, respectively. Between tumorous and medium density tissues, an average difference of 40% and 50% for the real and the imaginary part holds, respectively. The average difference reduces to 12% - 20% for the real and 22% - 28% for the imaginary part between tumorous and high density tissue. These results suggest that the higher the adipose content of adjacent normal tissue, the more significant the dielectric contrast of tumorous tissues that can be expected. In addition, for a given adipose content this contrast decreases with the frequency for the real part, although at 50 GHz it still remains larger than 10%, while it remains almost constant or slightly increasing with the frequency for the imaginary part.

In addition, Fig. 20 further details the discussion on the difference between tumorous and normal tissues including the information on the standard deviation, as already shown in Fig. 14 and Fig. 15, but in this case addressing each category of normal tissue separately. Therefore, while Fig. 14 and Fig. 15 address the situation where no *a-priori* information exists about the adipose content of the healthy tissues, Fig. 20 addresses the situation where such an information can be exploited. It can be observed that an overlap exists between tumorous and high-density normal tissues (Fig. 20a), while the separation against medium-density (Fig. 20b) and low-density (Fig. 2c) normal tissues roughly coincides or even greatly exceeds with the 1-sigma bands, respectively.

D. Analysis of the effects of patient age, sample temperature and time between excision and measurements

The patient age, the time between excision and measurement and the temperature of the sample during the measurement recorded for each sample are used to evaluate whether the dielectric properties of the breast tissues are statistically dependent on these parameters. In particular, the t-test is used for groups of the samples as described below, to determine if the sets of data are significantly different from each other. The tests are performed for several frequencies in order to span the whole frequency range.

Temperature effect

Because the dimensions of the measured samples are similar and the room temperature is tightly controlled, the temperature of the sample during the measurements remained stable, with a range limited to between 19°C and 22°C. According to the experience derived from the measurement of animal tissues, reported in Section II, this small variation does not provide any significant effect on the complex permittivity. For this reason, the temperature effect is not statistically evaluated.

Conversely, a larger temperature variation can affect the complex permittivity. This may be the case *in-vivo* conditions, where a temperature of around 37°C is to be expected. However, it is widely accepted that the dielectric properties of *ex-vivo* tissues can be seen as a worst case compared to *in-vivo* tissues in terms of contrast between normal and tumorous tissue, thus providing a conservative safe margin [12],[39].

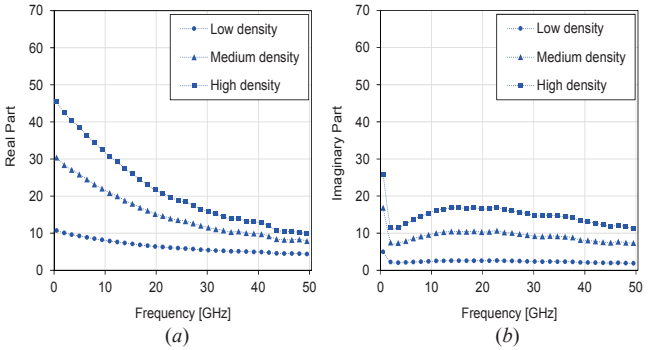

Figure 17. Comparison between the average real (a) and imaginary (b) part of the relative dielectric permittivity for different percentages of adipose content in normal tissues.

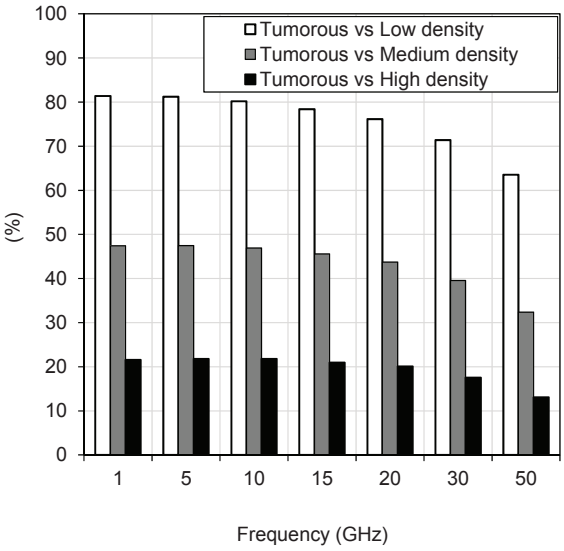

Figure 18. Percentage differences between the real part of the relative dielectric permittivity for tumorous and normal tissues.

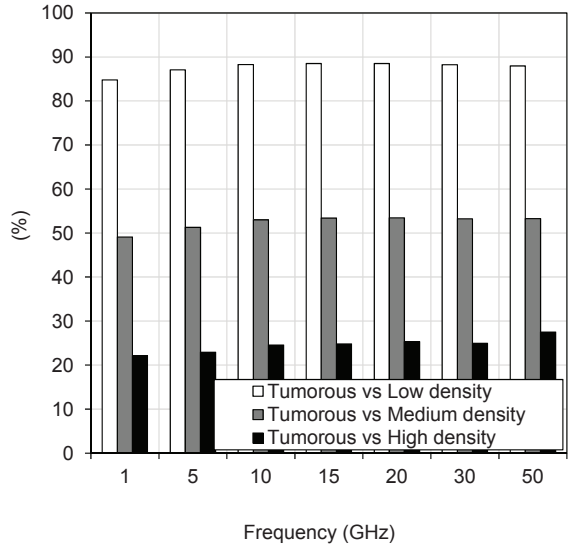

Figure 19. Percentage differences between the imaginary part of the relative dielectric permittivity for tumorous and normal tissues.

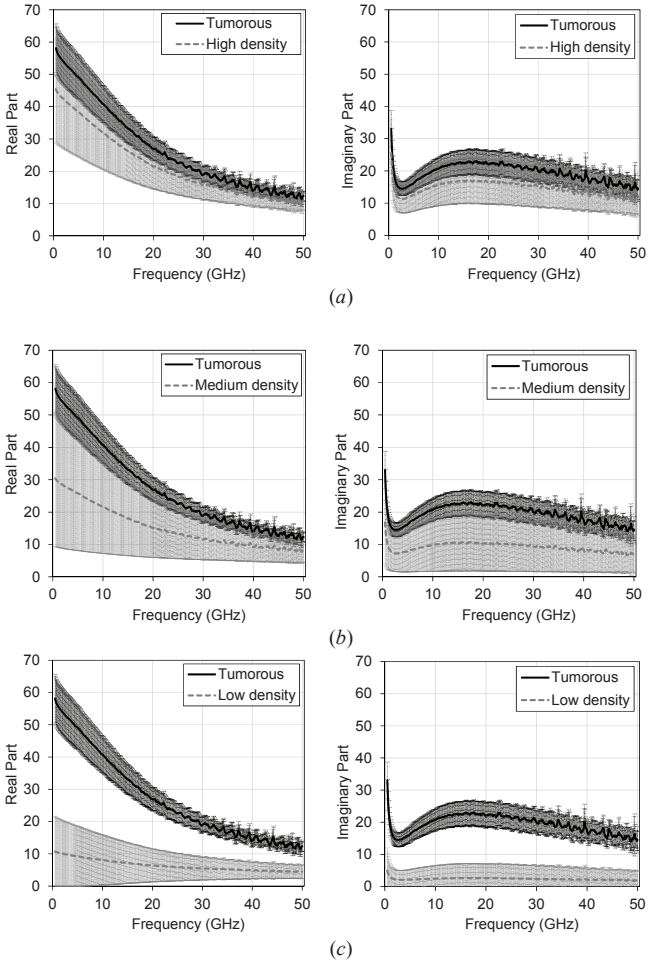

Figure 20. Comparison between the real (left column) and imaginary (right column) part of the relative dielectric permittivity between tumorous and normal tissues: (a) high density; (b) medium density; (c) low density. The black solid line depicts the average for tumorous tissues whereas the grey dashed line depicts the average for normal tissues. The shaded region denotes the variable range at ± 1 standard deviation.

Patient age

The effect of the patient age is analysed both for tumorous and normal tissues. The patients are divided into three groups, being the thresholds chosen to be relevant from a medical point of view:

1. age < 40 years;
2. age intermediate (≥ 40 years and ≤ 60 years);
3. age > 60 years.

The t-tests do not show any significant difference for tumorous tissues. Amongst the normal tissues, the age effect is evaluated using a t-test for each of the three groups based on the breast density. A significant differences is found only for the group with low density (80% - 100% of adipose tissue) between the youngest (age < 40 years) and oldest (age > 60 years) patients. For example, at 10 GHz, the average real and imaginary part of the relative permittivity are 11.6 and 4.25 for the younger group while they are 6.95 and 1.76 for the older group, and at 30 GHz the average real and imaginary parts are 7.1 and 4.1 for the younger group versus 5.06 and 1.74 for the older group.

Time between excision and measurements

The effect of the time between excision and measurements are analysed both for tumorous and normal tissues. The patients are divided in two groups:

1. time < 90 minutes;
2. time ≥ 90 minutes.

No significant difference is observed.

IV. Cole-Cole Models

The dielectric properties of biological tissues can be expressed through the Debye model [37], which allows to represent a wideband frequency-dependent dielectric spectrum through a compact and analytical representation. One of the most commonly used models is a modified version of the Debye expression, proposed in 1941 and named as Cole–Cole model. A single-pole Cole–Cole model based on the measurements is adopted in this work for representing the complex relative permittivity ε:

$$\varepsilon(\omega)=\varepsilon'(\omega)-j\varepsilon''(\omega)=\varepsilon_{\infty}+\frac{\Delta\varepsilon}{1+(j\omega\tau)^{1-\alpha}}+\frac{\sigma_S}{j\omega\varepsilon_0} \qquad (1)$$

where ε' and ε'' represent the frequency-dependent (through the angular frequency ω) real and imaginary part of the complex relative permittivity, and ε_∞, Δε, τ, α and σ_S are the Cole–Cole parameters, which are estimated through the least-square fitting to the measured average dielectric properties. The parameters obtained for tumorous and normal tissues, separated into three different categories (low, medium and high density), are reported in Table II and Table III.

Please note that Cole-Cole models are proposed for the measured average dielectric properties, thus representing the entire statistical population, not taking into account the different population age for the low-density normal tissues (the only case where differences were recorded). This choice is representative of a worst-case clinical situation, where no *a-*

priori information on the nature of the breast is available and thus general models should be used. A graphical depiction of the dielectric properties calculated over the 0.5 – 50 GHz range using the Cole-Cole model is compared with the corresponding averages of the measured values both for tumorous and normal tissues in Figs. 21 and 22. A good agreement over the entire frequency band is achieved both for the real and the imaginary part.

A comparison with the Cole–Cole parameters provided by previous experimental works below 20 GHz is presented in Table II and in Table III, for tumorous and normal tissues respectively [25],[26]. In addition a graphical representation is also shown in Figs. 21 and 22. It is worth noting that while both models can be virtually used at any frequency, above 20 GHz the previous model relies on extrapolations, while the model presented in this work is based on actual measurements. It can be observed that the two models (this work and [25], [26]) provide similar results up to 20 GHz for tumorous tissues and for normal tissues with a low adipose content, while the curves exhibit a difference for normal tissues with medium and high adipose content.

For tissues with high adipose contents (where even a modest water evaporation can significantly alter the tissue nature), a crucial role is the sample handling from surgery to microwave characterization, in particular in terms of humidity. As discussed in Sec. II, the clinical protocol agreed for this work minimized the water evaporation maintaining the larger excision always in bio-specimen transport bags and preparing the sample at the very last moment, exposing the sample itself to the air for less than one minute. Therefore, it is possible to partly approach the humidity condition typical of *in-vivo* tissues, which provides higher values for both the real and imaginary part [36]. For tissues with medium adipose contents the difference between the two models can be largely explained noting that this class of tissues includes samples within a wide range of adipose content (21-79 % and 31-84 % for this work and [25],[26], respectively). Consequently, the related curves are significantly dependent on the population distribution within these limits.

TABLE II – PARAMETERS OF THE COLE-COLE MODEL (1) FOR TUMOROUS TISSUES

	Tumorous (this work)	*Tumorous [25],[26]*
$\Delta\varepsilon$	50.5	50.09
ε_∞	5	6.749
τ(ps)	9	10.5
α	0.07	0.051
σ_S(S/m)	0.9	0.794

TABLE III – PARAMETERS OF THE COLE-COLE MODEL (1) FOR NORMAL TISSUES

Normal						
	Low density		*Medium density*		*High density*	
	This work[1]	*[25],[26]*[2]	*This work*[1]	*[25],[26]*[2]	*This work*[1]	*[25],[26]*[2]
$\Delta\varepsilon$	6	1.708	23	34.57	36.5	41.48
ε_∞	4	3.14	5	5.573	6	7.821
τ(ps)	10	14.65	19	9.149	9.4	10.66
α	0.09	0.061	0.08	0.095	0.06	0.047
σ_S(S/m)	0.1	0.036	0.5	0.524	0.7	0.713

[1]: Low density: 80 – 100 % of adipose tissue; Medium density: 20 – 80 % of adipose tissue; High density: 0 – 20 % of adipose tissue.
[2]: Low density: 85 – 100 % of adipose tissue; Medium density: 31 – 84 % of adipose tissue; High density: 0 – 30 % of adipose tissue.

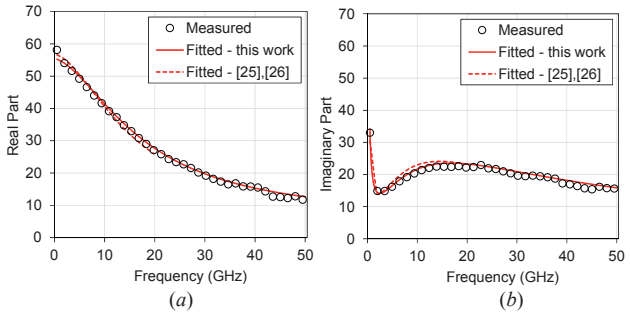

Figure 21. Measured and fitted (*a*) real part and (*b*) imaginary part of the relative dielectric permittivity for tumorous tissues. Comparison with the Cole-Cole model in [25], [26].

V. SENSITIVITY AND SPECIFICITY

The diagnostic performance of a given decision criteria can be characterized in terms of sensitivity (the percentage of sick people who are correctly identified as sick), and specificity (the percentage of healthy people who are correctly identified as healthy) [38]. Although a certain number of the diseased are correctly identified as such by a positive outcome of the test (true positive - Tp) some will be incorrectly classified as healthy (false negative - Fn), as shown in Fig. 23b.

In the same way, the healthy will be divided between those who are negative by the test (true negative - Tn) and those incorrectly classified by a positive result of the test (false positive - Fp). The values of sensitivity and specificity are related to the Tp, Fp, Tn and Fn values through the equations (2) and (3):

$$Sensitivity = \frac{Tp}{Tp + Fn} \tag{2}$$

$$Specificity = \frac{Tn}{Tn + Fp} \tag{3}$$

Ideally, both sensitivity and specificity would be 100%, with perfect distinction between the groups, as shown in Fig. 23a. In general, for real tests where Fp and Fn are always different from zero, the higher the sensitivity and the lower the specificity, and vice versa, depending on the choice of the decision threshold. In this study the sensitivity and specificity of mm-wave discrimination between tumorous and healthy *ex-vivo* tissue samples are calculated on the basis of a cut-off value defined by one standard deviation, which appear to provide a good separation between tumorous and normal tissues, as shown in Fig. 14 and in Fig. 15.

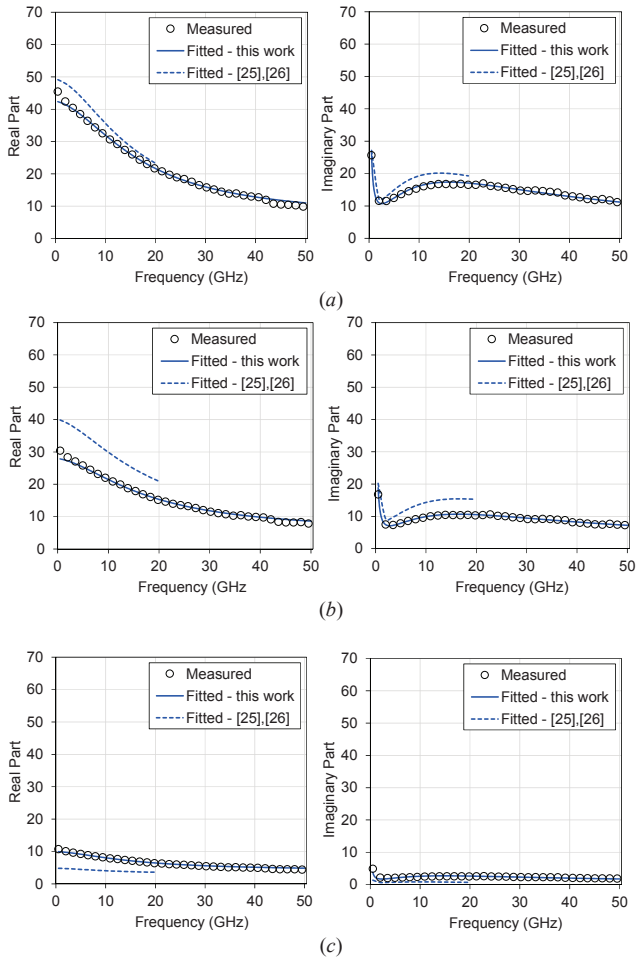

Figure 22. Measured and fitted real (left column) and imaginary (right column) part of the relative dielectric permittivity for normal tissues: (*a*) high density tissues; (*b*) medium density tissues; (*c*) low density tissues. Comparison with the Cole-Cole model in [25,26].

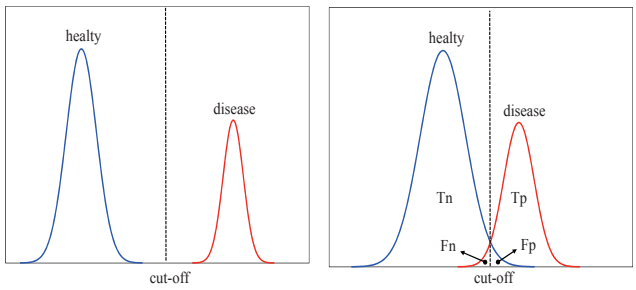

Figure 23. Example of an ideal test (a) and a real test (b) distribution.

The pathology findings were used as the definitive basis for tissue nature. Due to the distribution of the measurements, two different situations may occur during the evaluation of the sensitivity and specificity. In particular, to address the potential of the dielectric permittivity to work as the contrast parameter between normal and tumorous tissues, a fundamental pillar for all microwave and mm-wave applications, sensitivity and specificity are calculated at different frequencies (1 GHz, 5 GHz, 10 GHz, 15 GHz, 20 GHz, and 50 GHz) to highlight the frequency trend. In the first situation, which for example takes place at 1 GHz, the cut-off values of the two distributions (normal and tumorous tissues) do not overlap between them. In this case, as shown in Fig. 24, an undefined region is placed between the two cut-off values and the measurements that are located in this region are not considered in the calculation of sensitivity and specificity. In Table IV an example of values of Tp, Tn, Fp, and Fn derived for the real part of dielectric permittivity at 1 GHz is presented and in Table V the sensitivity and specificity calculated are reported. Conversely, in the second situation (for example at 50 GHz), the cut-off values of the two distributions overlap between them and an overlap region is identified, as shown in Fig. 25. In this case, the cut-off value of normal tissues is defined by the cut-off value calculated for tumorous tissues and conversely, the cut-off value of tumorous tissues is defined by the cut-off value calculated for normal tissues. In Table IV, an example of values of Tp, Tn, Fp, and Fn derived for the real part of dielectric permittivity at 50 GHz is presented and in Table V the sensitivity and specificity calculated are reported.

As anticipated, the values of sensitivity and specificity are calculated at different frequencies to emphasize the trend with the frequency, following the procedure described for the two situations.

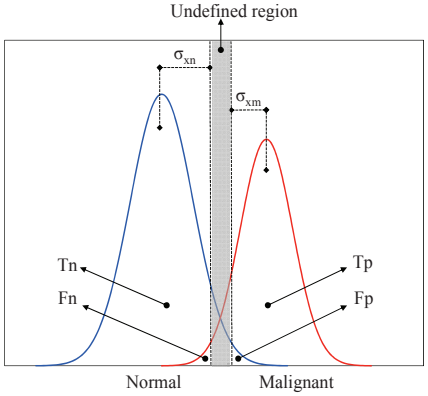

Figure 24. Situation in which the distributions of normal and tumorous tissues do not overlap between them. An example of results related to this situation is reported in Table IV for the frequency 1 GHz.

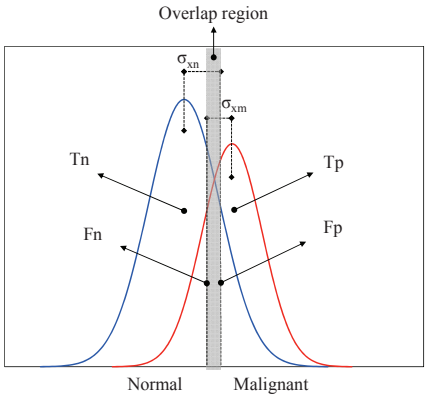

Figure 25. Situation in which the distributions of normal and tumorous tissues overlap between them. An example of results related to this situation is reported in Table IV for the frequency 50 GHz.

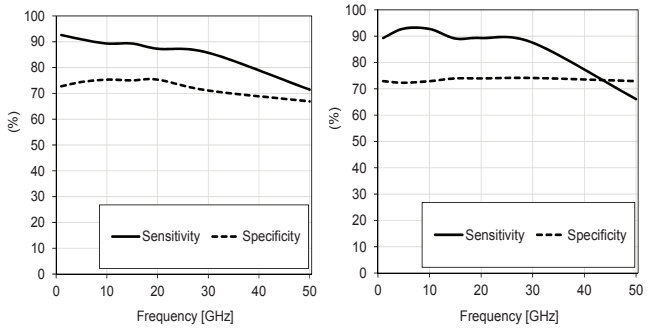

Figure 26. Sensitivity and specificity calculated for real (a) and imaginary (b) part of the relative dielectric permittivity.

TABLE IV – EXAMPLE OF SAMPLE DISTRIBUTION AT 1 GHZ AND 50 GHZ FOR THE REAL PART OF THE DIELECTRIC PERMITTIVITY

Frequency (GHz)	Test	Tumorous	Normal
1	Positive	50	45
	Negative	4	120
	Undefined	2	1
50	Positive	40	55
	Negative	16	111

TABLE V – EXAMPLE OF SENSITIVITY AND SPECIFICITY CALCULATED AT 1 GHZ AND 50 GHZ FOR THE REAL PART OF THE DIELECTRIC PERMITTIVITY

Frequency (GHz)	Sensitivity (%)	Specificity (%)
1	92.6	72.7
50	71.4	66.8

TABLE VI – COMPARISON BETWEEN MAMMOGRAPHY AND THE TEST BASED ON THE DIELECTRIC CHARACTERIZATION OF EX-VIVO BREAST TISSUES (AVERAGE BETWEEN REAL AND IMAGINARY PART, 0.5–50 GHZ)

Test	Sensitivity (%)	Specificity (%)
Mammography	75	85
This work	86.5	73

In Fig. 26 the parameters are shown both for the real (Fig. 26a) and imaginary (Fig. 26b) part of relative dielectric permittivity. It is worth noting that the specificity is practically stable, while the sensitivity decreases with frequency. Overall, this indicates that the relative contrast between normal and tumorous tissues is weaker at higher frequencies, although the sensitivity and specificity can be considered good up to at least 50 GHz. While the final sensitivity and specificity of a system intended to identify tumorous tissues from normal tissues is related to the actual frequency range adopted, in order to perform a global appraisal, the mean value between the real and imaginary part over the entire 0.5–50 GHz frequency range is calculated for both the sensitivity and specificity and reported in Table VI.

The results are in good agreement with typical values of sensitivity (70% - 80%) and specificity (80% - 90%) for the mammography, extrapolated from [39 – 41], with a slightly better sensitivity (i.e., the ability of correctly identifying tumorous tissues) and a slightly lower specificity (i.e., the ability of correctly identifying normal tissues).

Although this comparison is not intended for a direct benchmark of the different techniques, being this study based on *ex-vivo* tissues and the data on mammography on *in-vivo* cases, it represents a promising cornerstone to develop medical instruments at these frequencies.

VI. CONCLUSIONS

In this paper, the measured dielectric properties up to 50 GHz for 222 different breast tissue samples (156 normal and 56 tumorous samples) obtained from breast surgery were described. After the early preliminary measurements on animal tissues and a human breast presented in [29], this paper provides, for the first time beyond 20 GHz, a comprehensive study on a systematic database of measurements on human breast tissues.

The measurements, validated through pathological analysis showed that the dielectric properties of normal tissues are characterized by a wider variability than the tumorous tissues that appears due to heterogeneity in adipose content of different tissues within the healthy breast.

Despite this variability, tumorous tissues have significantly higher real and imaginary parts of the complex permittivity than normal breast tissues, providing a suitable contrast up to 50 GHz to enable future applications based on mm-waves, for both breast imaging and tissue identification during or after surgery. In addition, the effects of patient age and time between excision and measurements have a limited effect from the electromagnetic point of view, with age having an impact on the complex permittivity values only for the low-density normal tissues. The Cole-Cole models derived from measurements of tumorous and normal tissues aim to improve models of the electromagnetic response of breast tissues, including those used in full-wave simulators. This is essential for realistic investigation and development of medical systems and application in this frequency range, including mm-wave imaging systems.

The differences between normal and tumorous tissues were used to estimate the sensitivity and specificity (according to a standard method for pathological analysis, as defined in Section V) of a test based on the dielectric characterization of *ex-vivo* tissues. The diagnostic performance is comparable to that of mammography performed *in*-vivo on patients. While not directly comparable because of the differences between *ex-vivo* and *in-vivo* tissues, this is a positive indication for future developments of medical instruments applying mm-waves frequencies.

VII. ACKNOWLEDGMENT

The authors would like to thank Simona Di Meo, Alesja Delisina and all gross-pathology staff of the European Institute of Oncology for their help during the experimental campaign.

REFERENCES

[1] F. Töpfer and J. Oberhammer, "Millimeter-wave tissue diagnostics: the most promising fields for medical applications," *IEEE Microwave Magazine*, Vol. 16, No. 4, pp. 97-113, May 2015.

[2] W. J. Fleming, "Forty-year review of automotive electronics," *IEEE Vehicular Technology Magazine*, Vol. 10, No. 3, pp. 80-90, September 2015.

[3] S. S. Ahmed, A. Genghammer, A. Schiessl, and L.-P. Schmidt, "Fully electronic E-band personnel imager of 2 m² aperture based on a multistatic architecture," *IEEE Transactions on Microwave Theory and Techniques*, Vol. 61, No. 1, pp. 651-657 January 2013.

[4] J. Antes and I. Kallfass, "Performance estimation for broadband multi-gigabit millimeter- and sub-millimeter-wave wireless communication links," *IEEE Transactions on Microwave Theory and Techniques*, Vol. 63, No. 10, pp. 3288-3299 January 2013.

[5] E. C. Fear, S. C. Hagness, P. M. Meaney, M. Okoniewski, and M. A. Stuchly, "Enhancing breast tumor detection with near-field imaging," *IEEE Microwave Magazine*, Vol. 3, No. 1, pp. 48–56, March 2002.

[6] P. T. Nguyen, A. Abbosh, and S. Crozier, "Microwave hyperthermia for breast cancer treatment using electromagnetic and thermal focusing tested on realistic breast models and antenna arrays," *IEEE Transactions on Antennas and Propagation*, Vol. 63, No. 10, pp. 4426-4434 October 2015.

[7] M. Hofmann, G. Fischer, R. Weigel, and D. Kissinger, "Microwave-based noninvasive concentration measurements for biomedical applications," *IEEE Transactions on Microwave Theory and Techniques*, Vol. 61, No. 5, pp. 2195–2204, May 2013.

[8] D. Bennett, Z. Taylor, P. Tewari, S. Sung, A. Maccabi, R. Singh, M. Culjat, W. Grundfest, J.-P. Hubschman, and E. Brown, "Assessment of corneal hydration sensing in the terahertz band: In vivo results at 100 GHz," *Journal of Biomedical Optics*, Vol. 17, No. 9, pp. 097008-1–097008-7, September 2012.

[9] Y. Nikawa, N. Hoshi, K. Kawai, and S. Ebisu, "Study on dental diagnosis and treatment using millimeter waves," *IEEE Transactions on Microwave Theory and Techniques*, Vol. 48, No. 11, pp. 1783–1788, November 2000.

[10] A. Taeb, S. Gigoyan, and S. Safavi-Naeini, "Millimetre-wave waveguide reflectometers for early detection of skin cancer," *IET Microwaves, Antennas and Propagations*, Vol. 7, No. 14, pp. 1182–1186, November 2013.

[11] T. Wu, T. S. Rappaport, and C. M. Collins, "Safe for generations to come: considerations of safety for millimeter waves in wireless communications," *IEEE Microwave Magazine*, Vol. 16, No. 2, pp. 65–84, March 2015.

[12] N. K. Nikolova, "Microwave imaging for breast cancer," *IEEE Microwave Magazine*, Vol. 12, No. 7, pp. 78–94, December 2011.

[13] M. Klemm, I. J. Craddock, J. A. Leendertz, A. Preece, and R. Benjamin, "Radar-based breast cancer detection using a hemispherical antenna array - experimental results," *IEEE Transactions on Antennas and Propagation*, Vol. 57, No. 6, pp. 1692–1704, June 2009.

[14] T. M. Grzegorczyk, P. M. Meaney, P. A. Kaufman, R. M. diFlorio-Alexander and, K. D. Paulsen "Fast 3-D tomographic microwave imaging for breast cancer detection," *IEEE Transactions on Medical Imaging*, Vol. 31, No. 8, pp. 1584–1592, August 2012.

[15] E. C. Fear, J. Bourqui, C. Curtis, D. Mew, B. Docktor, and C. Romano, "Microwave breast imaging with a monostatic radar-based system: a study of application to patients," *IEEE Transactions on Circuits and Systems*, Vol. 61, No. 5, pp. 2119–2128, May 2013.

[16] M. J. Burfeindt, J. D. Shea, B. D. Van Veen, and S. C. Hagness, "Beamforming-Enhanced inverse scattering for microwave breast imaging," *IEEE Transactions on Antennas and Propagation*, Vol. 62, No. 10, pp. 5126–5132, June 2009.

[17] H. Bahramiabarghouei, E. Porter, A. Santorelli, B. Gosselin, M. Popovic, and L. A. Rusch, "Flexible 16 antenna array for microwave breast cancer detection," *IEEE Transactions on Biomedical Engineering*, Vol. 62, No. 10, pp. 2516–2525, October 2015.

[18] M. Klemm, I. J. Craddock, and,A. W. Preece, "Contrast-enhanced breast cancer detection using dynamic microwave imaging," *IEEE Antennas and Propagation Society International Symposium*, Chicago, U.S.A., July 8–14, 2012.

[19] S. Moscato, G. Matrone, M. Pasian, A. Mazzanti, M. Bozzi, L. Perregrini, F. Svelto, G. Magenes, P. Arcioni, and P.E. Summers, "A mm-Wave 2D ultra-wideband imaging radar for breast cancer detection," *International Journal of Antennas and Propagation*, Vol. 2013, Article ID 475375, 8 pages, 2013.

[20] M. Bassi, M. Caruso, M. S. Khan, A. Bevilacqua, A. D. Capobianco, and A. Neviani, "An integrated microwave imaging radar with planar antennas for breast cancer detection," *IEEE Transactions on Microwave Theory and Techniques*, Vol. 61, No. 5, pp. 2108–2118, May 2013.

[21] L. Chao, M. Afsar, and K. Korolev, "Millimeter wave dielectric spectroscopy and breast cancer imaging," in *2012 7th European Microwave Integrated Circuits Conference (EuMIC)*, Amsterdam, The Netherlands, October 28 – November 2, 2012.

[22] C. Yu, S. Fan, Y. Sun, and E. Pickwell-MacPherson, "The potential of terahertz imaging for cancer diagnosis: a review of investigations to date," *Quantitative Imaging in Medicine and Surgery*, Vol. 2 , No. 1, pp. 33–45, March 2012.

[23] S. J Erickson-Bhatt, M. Roman, J. Gonzalez, A. Nunez, R. Kiszonas, C. Lopez-Penalver, and A. Godavarty, "Noninvasive surface imaging of breast cancer in humans using a hand-held optical imager," *Biomedical Physics and Engineering Express*, Vol. 1, pp. 045001-1–045001-11, 2015.

[24] A. Fitzgerald, V. Wallace, M. Jimenez-Linan, L. Bobrow, R. Pye, A. Purushotham, and D. Arnone, "Terahertz pulsed imaging of human breast tumors," *Radiology*, Vol. 239, No. 2, pp. 533–540, May 2006.

[25] M. Lazebnik, *et al*., "A large-scale study of the ultrawideband microwave dielectric properties of normal breast tissue obtained from reduction surgeries," *Physics in Medicine and Biology*, Vol. 52, No. 10, pp. 2637–2656, 2007.

[26] M. Lazebnik, *et al*., "A large-scale study of the ultrawideband microwave dielectric properties of normal, benign and malignant breast tissues obtained from cancer surgeries," *Physics in Medicine and Biology*, Vol. 52, No.20, pp. 6093–6115, 2007.

[27] P. Ashworth, E. Pickwell-MacPherson, E. Provenzano, S. Pinder, A. Purushotham, M. Pepper, and V. Wallace, "Terahertz pulsed spectroscopy of freshly excised human breast cancer," *Optics Express*, vol. 17, no. 15, pp. 12444-12454, 2009.

[28] B. C. Q. Truong, H. D. Tuan, A. J. Fitzgerald, V. P. Wallace, and H. T. Nguyen, "A Dielectric model of human breast tissue in terahertz regime," *IEEE Transactions on Biomedical Engineering*, Vol. 62, No. 2, pp. 699–707, February 2015.

[29] A. Martellosio, M. Pasian, M. Bozzi, L. Perregrini, A. Mazzanti, F. Svelto, P.E. Summers, G. Renne, and M. Bellomi, "0.5–50 GHz dielectric characterization of breast cancer tissues," *IET Electronics Letters*, Vol. 51, No. 13, pp. 974–975, June 2015.

[30] M. Stuchly and S. Stuchly, "Coaxial line reflection methods for measuring dielectric properties of biological substances at radio and microwave frequencies—A review," *IEEE Transactions on Instrumentation & Measurement*, Vol. 29, No. 3, pp. 176–183, September 1980.

[31] P. M. Meaney, A. P. Gregory, N. R. Epstein, and K. D. Paulsen, "Microwave open-ended coaxial dielectric probe: interpretation of the sensing volume re-visited," *BMC Medical Physics*, Vol. 14, No. 3, pp. 1756-6649-1–1756-6649-11, 2014.

[32] R. J. Sengwa, "Comparative dielectric study of mono, di and trihydric alcohols," *Indian Journal of Pure & Applied Physics*, Vol. 41, pp. 295–300, April 2003.

[33] F. Buckley and A. Allen Maryott, *Tables of dielectric dispersion date for pure liquids and dilute solutions*, U.S. Dept. of Commerce, National Bureau of Standards, November 1958.

[34] A.Boughriet, Z.Wu, H. McCann, and L.E. Davis, "The measurement of dielectric properties of liquids at microwave frequencies using open-ended coaxial probes," 1st World Congress on Industrial Process Tomography, Buxton, Greater Manchester, UK, April 14–17, 1999.

[35] D. K. Ghodgaonkar, Y. V. Varadan, and Y. K. Varadan, "A free-space method for measurement of dielectric constants and loss tangents at microwave frequencies," *IEEE Transactions on Instrumentation and Measurement*, Vol. 37, No. 3, pp. 789–793, June 1989.

[36] R. J. Halter, T. Zhou, P. M. Meaney, A. Hartov, R. J. Barth, Jr, K. M. Rosenkranz, W. A. Wells, C. A. Kogel, A. Borsic, E. J. Rizzo, and K. D. Paulsen, "The correlation of in vivo and ex vivo tissue dielectric properties to validate electromagnetic breast imaging: initial clinical experience," *Physiol Meas.*, Vol. 30, No. 6, pp. 0967-3334-1–0967-3334-23, June 2009.

[37] C. Gabriel, *Dielectric properties of biological materials*, Chapter 3 in 'Handbook of Biological Effects of Electromagnetic Field', CRC Press, 2006.

[38] A. G. Lalkhen and A. Y. McCluskey, "Clinical tests: sensitivity and specificity," *Continuing Education in Anaesthesia, Critical Care & Pain*, Vol. 8, No. 6, pp. 221–223, 2008.
[39] S. Hofvind , B. M. Geller, J. Skelly, and P. M. Vacek, "Sensitivity and specificity of mammographic screening as practised in Vermont and Norway," *British Journal of Radiology*, Vol. 85, No. 1020, pp. 1226–1257, December 2012.
[40] A. M. Kavanagh, G. G. Giles, H. Mitchell, and J. N. Cawson. "The sensitivity, specificity, and positive predictive value of screening mammography and symptomatic status," *Journal of Medical Screening*, Vol. 7, No. 2, pp. 105–114, 2000.
[41] R. Ferrini, E. Mannino, E. Ramsdell, and L. Hill, "Screening mammography for breast cancer: American college of preventive medicine practice policy statement," *American Journal of Preventive Medicine*, Vol. 12, No. 5, pp. 340–344, Sept.–Oct. 1996.

Andrea Martellosio (S'14) was born in Lodi, Italy, in 1988. He received the M.S. degree in electronic engineering from the University of Pavia, Pavia, Italy, in 2013. From January 2014 he joined the European Institute of Oncology (IEO) as research fellow for which his work was focused on the 3D imaging for breast cancer detection using millimetre and sub-millimetre waves. Currently he is working toward the Ph.D. degree in electronics at the University of Pavia and his research activities are focused on the study and development of microwave and millimetre wave antenna systems.

Marco Pasian (S'06–M'09–SM'15) was born in 1980. He received the M.Sc. degree (*cum laude*) in electronic engineering and the Ph.D. in electronics and computer science from the University of Pavia, Pavia, Italy, in 2005 and 2009, respectively.
Since 2013 he has been a Research Fellow of the Microwave Laboratory at the University of Pavia, where he held a position as PostDoc from 2009 to 2013. He was with the European Space Agency, Germany, with Carlo Gavazzi Space, Italy and with the TNO, Defence, Security and Safety, The Netherlands in 2004, 2005 and 2008, respectively. He is an Associate Editor of the European Microwave Association (EuMA) INTERNATIONAL JOURNAL OF MICROWAVE AND WIRELESS TECHNOLOGIES.
Dr. Pasian was the Technical Program Co-Chair of the European Microwave Conference 2014, the Conference Prize Committee Chair of the European Microwave Week 2014, and the Finance Chair of the IEEE International Conference on Numerical and Electromagnetic Modeling and Optimization (NEMO 2014). He was a recipient of a competitive grant from the Italian Ministry of Education, University, and Research under the funding schema Scientific Independence of Young Researchers (SIR2104). He is member of the EuMA.

Maurizio Bozzi (S'98–M'01–SM'12) was born in Voghera, Italy, in 1971. He received the Ph.D. degree in electronics and computer science from the University of Pavia, Pavia, Italy, in 2000.
He held research positions with various universities worldwide, including the Technische Universität Darmstadt, Germany; the Universitat de Valencia, Spain; and the École Polytechnique de Montréal, Canada. In 2002, he joined the Department of Electronics, University of Pavia, where he is currently an Associate Professor. He is also a Guest Professor of the Tianjin University (China) for the term 2015-2017.
He has authored or co-authored more than 90 journal papers and 250 conference papers. He co-edited the book Periodic Structures (Research Signpost, 2006) and co-authored the book Microstrip Lines and Slotlines (Artech House, 2013). His main research interests concern the computational electromagnetics, the substrate integrated waveguide technology, and the use of novel materials and fabrication technologies for microwave circuits (including paper, textile, and 3D printing).
Prof. Bozzi is the 2016 Secretary of the IEEE Microwave Theory and Techniques Society (MTT-S), an elected member of the Administrative Committee of the IEEE MTT-S for the term 2017–2019, and a member of the General Assembly (GA) of the European Microwave Association (EuMA) for the term 2014–2016. He is an associate editor for the IEEE MICROWAVE AND WIRELESS COMPONENTS LETTERS, the IET Electronics Letters, and the IET Microwaves, Antennas and Propagation. He was the General Conference Chair of the IEEE International Conference on Numerical Electromagnetic Modeling and Optimization, NEMO2014, Pavia, Italy, 2014, and the General Chair of the IEEE MTT-S International Microwave Workshop Series on Millimeter Wave Integration Technologies, Sitges, Spain, 2011.
He received several awards, including the 2015 Premium Award for Best Paper in IET Microwaves, Antennas & Propagation, the 2014 Premium Award for the Best Paper in Electronics Letters, the Best Young Scientist Paper Award of the XXVII General Assembly, URSI, in 2002, and the MECSA Prize of the Italian Conference on Electromagnetics (XIII RiNEm), in 2000.

Luca Perregrini (M'97-SM'12-F'16) was born in Sondrio, Italy, in 1964. He received the "Laurea" degree in Electronic Engineering and the Ph.D. in Electronics and Computer Science in 1989 and 1993, respectively. In 1992 he joined the Faculty of Engineering of the University of Pavia, he is now full professor of electromagnetic fields and responsible of the Microwave Laboratory. He has been the tutor of several Ph.D. students and the supervisor of many MS and BS students. He has been a visiting professor at the École Polytechnique de Montréal, Québec, Canada in 2001, 2002, 2005, and 2006.
Prof. Perregrini has been responsible of many research contracts with prominent international research centers and companies. His main research interests have been focused on the development of numerical methods for electromagnetics, and the design of microwave components and antennas.
He is Fellow of the Institute of Electrical and Electronics Engineers (IEEE), a member of the Technical Committee MTT–15 (Microwave Field Theory) of IEEE MTT Society, member of the Board of Directors of the European Microwave Association (EuMA), member of the Società Italiana di Elettromagnetismo (SIEm), and he has been a member of the General Assembly of EuMA (2011-2013).
Prof. Perregrini is currently Editor in Chief of the IEEE TRANSACTIONS ON MICROWAVE THEORY AND TECHNIQUE. He also serves as Associate Editor of the International Journal of Microwave and Wireless Technologies (since 2011), IET Electronic Letters (since 2015), and of the International Journal of Microwave and Wireless Technologies (June 2015). He was Associate Editor of the IEEE MICROWAVE AND WIRELESS COMPONENTS LETTERS (2010-2013) and of IEEE TRANSACTIONS ON MICROWAVE THEORY AND TECHNIQUES (2013-2016)), and Gest Editor of the IEEE TRANSACTIONS ON MICROWAVE THEORY AND TECHNIQUES (Jan. 2015). He co-edited the book Periodic Structures, (Research Signpost, 2006). He is the appointed General Conference Chair of the European Microwave Week 2020 (Rome, Italy), the Technical Program Committee Chair of the International Microwave Workshop Series on Advanced Materials and Processes (IMWS-AMP 2017) (Pavia, Italy, Sept. 2017), and he was the Technical Program Committee Chair of the IEEE MTT-S International Conference on Numerical Electromagnetic Modeling and Optimization (NEMO2014) (Pavia, Italy, May 2014), and of the European Microwave Conference (Rome, Italy, Oct. 2014). He also served as a member of prize committees for several conferences/societies.
Prof. Perregrini has been an invited speaker at many conferences, and has delivered invited seminar talks in Universities and research centers worldwide. He was the co-recipient of the Best Paper Award at the 15th Mediterranean Microwave Symposium (MMS2015), of the Best Student Paper Award at the 4th European Conference on Antennas and Propagation (EuCAP 2010), and the 2nd Best Student Paper Award at the 27th Int. Review of Progress in Applied Computational Electromagnetics (ACES 2010). He authored or co-authored more than 80 journal papers and more than 230 conference papers, 6 book chapters, and 2 textbooks.

Andrea Mazzanti (S'02–M'09–SM'13) received the Laurea and Ph.D. degrees in electrical engineering from the Università di Modena and Reggio Emilia, Modena, Italy, in 2001 and 2005, respectively. During the summer of 2003, he was with Agere Systems, Allentown, PA as an Intern. From 2006 to 2009, he was Assistant Professor with the Università di Modena and Reggio Emilia. In January 2010, he joined the Università di Pavia where he is now Associate Professor. He has

authored over 90 technical papers. His main research interests cover device modeling and IC design for high-speed communications, RF and millimeter-wave systems. Dr. Mazzanti has been a member of the Technical Program Committee of the IEEE Custom Integrated Circuit Conference (CICC) from 2008 to 2014, IEEE European Solid State Circuits Conference (ESSCIRC) and IEEE International Solid State Circuits Conference (ISSCC) since 2014. He has been Associate Editor for the Transactions on Circuits and Systems-I from 2012 to 2015 and Guest Editor for special issues of the Journal of Solid State Circuits dedicated to CICC 2013-14 and ESSCIRC-2015.

Francesco Svelto (S'93–M'98–SM'11–F'13) received the Laurea and Ph.D. degrees in electrical engineering from Università di Pavia, Pavia, Italy, in 1991 and 1995, respectively.
During 1995–1997, he held an industry grant for research in RF CMOS. In 1997 he was appointed Assistant Professor at Università di Bergamo, and in 2000, he joined Università di Pavia, where he is now Professor and Vice-Rector for knowledge transfer. He has been technical advisor of RFDomus Inc., a start-up he cofounded in 2002dedicated to highly integrated GPS receivers. After merging with Glonav Inc. (Ireland), RFDomus has been acquired by NXP Semiconductors in 2007. Since 2006 he has been the Director of a Scientific Laboratory, joint between Università di Pavia and STMicrolectronics, dedicated to research in Microelectronics, with emphasis to mm-wave systems for wireless communications, high-speed serial links and ultrasound electronics for medical diagnostic.
Dr. Svelto has been a Member of the technical program committee of the International Solid State Circuits Conference, the Custom Integrated Circuits Conference, and the Bipolar/BiCMOS Circuits Technology Meeting. He is presently a Member of the technical program committee of IEEE European Solid State Circuits Conference. He served as Associate Editor of the IEEE JOURNAL OF SOLID-STATE CIRCUITS (2003–2007), and as Guest Editor for a special issue on the same journal in March 2003. He is co-recipient of the IEEE JOURNAL OF SOLID-STATE CIRCUITS 2003 Best Paper Award. Presently, he is Fellow of the International Institution for Electrical and Electronics Engineering and Solid State Circuits Society Distinguished lecturer.

Paul E. Summers received B.S. degrees in physics and mathematics from the University of Alberta, Edmonton, Canada, in 1987 and 1989, respectively, and the Ph.D. degree from King's College - University of London, London, UK, in 1999.
He is a Researcher at the European Institute of Oncology (IEO) and at the Fondazione IRCSS Ca Granda Ospedale Maggiore Policlinico. Milan, Italy. His current research interests include application of magnetic resonance imaging in oncology, neuroradiology and neuroscience, and the medical applications of millimeter waves.
Dr. Summers is a member of ISMRM, ESMRMB, AIFM and IPEM.

Giuseppe Renne was born on April 10th, 1957 in Cosenza (Italy) and educate in Italy, where he graduated from Medical School at the State University of Naples (II° Faculty) in 1981. Postgraduate training was performed at Department of Pathology of Niguarda Cà Granda Hospital of Milan and at UCSC – Policlinico "A. Gemelli" of Rome.He obtained at the Cattolica University "Sacro Cuore"of Rome his Specialization degree in Anatomic Pathology. His areas of interest include breast cancer, uropathology and diagnostic cytology.
He became deputy director at Service of Surgical Pathology, Regional Hospital, Magenta on 1995 and at Service of Surgical Pathology, S. Carlo B. Hospital, Milan on 1998. Since 1999 he is deputy director and since 2002 senior deputy director at the Dept. of Pathology and Laboratory Medicine of the European Institute of Oncology in Milan. Since 2007 he is codirector at Dept. of Pathology of IEO. Since 2015 he is director of Uropathology and Intraoperative Diagnostic Unit at the European Institute of Oncology in Milan. He is co-author of more than 80 publications in peer-reviewed journal.

Lorenzo Preda was Born in Pavia, 9th April 1964. He received the Degree in Medicine and Surgery in 1989 and the Postgraduate specialization in Radiology from the University of Pavia, Pavia, Italy. He held positions as Assistant at the Institute of Radiology of IRCCS Policlinico San Matteo, Pavia, Italy (1991-2001), as Adjunct professor at the Postgraduate school of the specialization in Radiology of the Medicine and Surgery Faculty, University of Pavia, Pavia, Italy (1996-1997 and 2015-2016). Since 2006 he has been Senior Deputy Director at the Division of Radiology of the European Institute of Oncology, Milan, Italy, since 2016 Associate Professor at the Department of Clinical-Surgical, Diagnostic and Pediatric Sciences, University of Pavia, Pavia, Italy, and since 2016 Director at the Radiology Unit of the National Center of Oncological Hadrontherapy (CNAO Foundation), Pavia, Italy.
He has authored or co-authored about 90 papers.
Prof. Preda was a member of the Scientific Editorial Board of European Radiology from 2008 to 2014, and he has been Board member of the Odontostomatological and Head-Neck Radiology Section of SIRM since 2012 and Board member of the Italian Association of Cervico-Cephalic Oncology (AIOCC) since 2015. He was the recipient of the Fellowship of the European Society of Head and Neck Radiology in 2013.

Massimo Bellomi graduated in Medicine and Surgery at the University of Milan in 1975. In 1976 he specialized in Hepatology and in 1980 he obtained a second Postgraduate Diploma in Radiology and Radiotherapy. From 1980 he received several research grants for studies on liver and gastrointestinal pathologies: at the University Hospital of Pennsylvania (1980), Thomas Jefferson University of Philadelphia (1980), and at University of Lund, Sweden (1983).
He was part of the team which introduced Percutaneous Biliary Drainage and Gastrointestinal Interventional Radiology in Italy and developed a number of techniques for Interventional and Diagnostic Radiology. He also designed software for archiving radiologic examinations and for image processing and analysis. In 1984, 1988 and 1991 he was appointed Director of Operative Units and research projects in Oncology of the National Research Council. In 1994 he became Director of the Department of Radiology of the European Institute of Oncology in Milan. In 1998 he became Associate Professor of Radiology of the Department of Health Sciences, University of Milan. From 2000 to 2003 he was a member of the Ministry of Health Commission for studies in Diagnostic Imaging. In 2000-2003 and 2009-2012 he was Director of the postgraduated School of Radiology of the School of Medicine, University of Milan. In 2012 he was appointed as President of the School in Imaging and Radiotherapy Techniques, University of Milan. He is principal investigators in a numbers of clinical trials and author of 238 scientific publications; 23 of them are book chapter. He is Editor of European Journal of Radiology and Cancer Imaging Journal.
Prof. Bellomi is member of several scientific societies including SIRM Italian Society of Radiology, ICIS International Cancer Imaging Society (Founding member and President in 2033-2004), ESR European Society of Radiology.